

SANS Studies of Liquid–Liquid Phase Separation in Heterogeneous and Metallocene-Based Linear Low-Density Polyethylenes

G. D. Wignall,^{*,†} R. G. Alamo,^{*,‡} E. J. Ritchson,[‡] L. Mandelkern,[§] and D. Schwahn[⊥]

Solid State Division, Oak Ridge National Laboratory,[#] Oak Ridge Tennessee 37831; Chemical Engineering Department, Florida A&M University and Florida State University College of Engineering, Tallahassee, Florida 32310-6046; Department of Chemistry, Florida State University, Tallahassee, Florida 32306; and Institute für Festkörperforschung, Forschungszentrum, Jülich D-52425, Germany

Received April 23, 2001

ABSTRACT: An ethylene–hexene copolymer, representative of many heterogeneous linear low-density polyethylenes (LLDPEs), has been shown to contain a dispersed minority phase (volume fraction $\sim 10^{-2}$), which was manifested by departures from a Q^{-2} variation of the neutron scattering cross section at low Q values. After xylene extraction, which removes the highly branched amorphous material, the dispersed phase is removed to a good approximation. In contrast, a metallocene-based LLDPE, which has a more homogeneous distribution of branch contents, does not exhibit an upturn in the cross section in the limit of low momentum transfer ($Q < 10^{-2} \text{ \AA}^{-1}$), indicating that the LLDPE forms only a single phase in the melt. The composition variance is calculated from the comonomer composition distribution obtained by temperature-rising elution fractionation (TREF) and used to estimate proximity of the melts to the spinodal condition. These findings support previous conclusions for compositionally polydisperse LLDPEs, whereby the highly branched molecules in the distribution may phase segregate, even if the overall branch content is low. When this component is not present, as in metallocene-based LLDPEs, the system forms a single phase in the melt.

Introduction

It is well established^{1–10} that small-angle neutron scattering (SANS) can be used to determine the melt compatibility of mixtures of linear and branched polyolefins, including high density (HD), low density (LD), and linear low density (LLD) polyethylene (PE). HDPE chains contain very little branching, though LDPE contains some short chain branches (1–3 per 100 backbone carbon atoms) as well as a few long chain branches (< 0.3 per 100 backbone carbon atoms). Linear low density polyethylene (LLDPE) is produced by catalytically copolymerizing ethylene with an α -olefin (e.g., hexene, octene, etc.) and can have a wide range of branch contents, depending on the type of catalyst and concentration of added comonomer, with a homogeneous side (short) branch length. SANS indicates that for HDPE/LDPE blends with molecular weights $\sim 10^5$ the melt is homogeneous for all compositions after proper accounting for H/D isotope effects,^{1,2} in the size range normally probed via pinhole cameras (10^1 – 10^3 \AA) and also on micrometer length scales.⁹ Similarly, SANS indicates^{3–6} that mixtures of HDPE and LLDPE are homogeneous in the melt when the branch content is low (i.e., < 3 branches/100 backbone carbons). However, when the branch content is higher (> 10 branches/100C), the blends phase separate.^{5,6}

In previous SANS experiments,^{3–6} the LLDPEs were simulated by hydrogenated (or deuterated) polybutadienes, because these materials may be prepared as nearly monodisperse ($M_w/M_n < 1.1$) molecules with a

homogeneous branch distribution within each chain. Thus, these studies were not affected by polydispersity effects, in either the branch content or molecular weight. However, for LLDPEs prepared with heterogeneous-type Ziegler–Natta catalysts, it is well-known that the multisite nature of catalysts typically leads to a wide distribution of chain compositions.¹¹ The branch content and molecular weight are strongly correlated, and the low molecular weight chains exhibit the most branching.^{12,13}

Thus, a heterogeneous LLDPE may be thought of as a “blend” of different species, and when the composition distribution is broad enough, the multicomponent system can, in principle, phase separate, as suggested by Mirabella,¹³ Debliek,¹⁴ and co-workers and substantiated by scanning electron microscopy (SEM) investigations of the solid state.^{13,15} In addition, Nesarikar et al.¹⁵ performed a thermodynamic calculation of the equilibrium melt state using a distribution of chain branching estimated from temperature rising elution fractionation (TREF)^{12,13} and predicted a small fraction (~ 0.02) of a second phase consisting of highly branched amorphous material, in reasonable agreement with the SEM findings.^{13,15}

Wignall and co-workers⁷ performed complementary SANS studies to examine the structure of the melt directly. Because the linear and branched molecules have virtually the same scattering power, there is no contrast between the phases and the melt structure would not be manifested via X-ray or light scattering, so a fraction of deuterated linear polymer (20%) was added. On the basis of previous studies, the linear material should be incompatible with the minority phase but should mix homogeneously with the predominantly low branched matrix. Thus, the addition of HDPE-D provided SANS contrast and allowed direct determination of the predicted two-phase morphology, and by this means it was shown that an ethylene–

[†] Oak Ridge National Laboratory.

[‡] Florida A&M University and Florida State University College of Engineering.

[§] Florida State University.

[⊥] Institute für Festkörperforschung.

[#] Managed by UT-Battelle, LLC, under Contract DE-AC05-00OR22725 with the U. S. Department of Energy.

* Corresponding authors.

Table 1. Characterization of Ziegler–Natta Ethylene–Hexene (EH), Metallocene Ethylene–Octene (EO) Copolymers, and Deuterated Linear Polyethylene Used To Provide SANS Contrast

sample	$10^{-3}M_w$	$10^{-3}M_n$	branches/100 backbone C or mol % branches
Ziegler–Natta EH	120	30	1.7
metallocene EO	84.5	38.4	1.5
deuterated HDPE	115.4	21.2	

hexene (EH) copolymer, representative of many LLDPEs, contained a dispersed minority phase (volume fraction, $\phi \sim 10^{-2}$), as predicted.^{13–15} The dispersed phase was eliminated to a good approximation by xylene extraction, which removed the highly branched molecules. The extracted material contains a much higher fraction of branched molecules and hence has a greater proportion of the dispersed phase ($\phi \sim 0.2$). These findings supported the prediction of liquid–liquid phase separation for compositionally polydisperse LLDPEs, whereby the more highly branched molecules in the distribution phase segregate, even if the overall branch content is low. Conversely, LLDPEs produced by single site, metallocene catalysts should have a much more homogeneous distribution of branch contents and would not be expected to show such a two-phase morphology. It is the purpose of this study to compare Ziegler–Natta and metallocene-based LLDPEs to test this prediction.

Sample Preparation and Characterization

The molecular weight and branch composition were analyzed by conventional GPC and ^{13}C NMR techniques for the Ziegler–Natta-based ethylene–hexene (EH) copolymer studied previously^{7,9} and also a metallocene-catalyzed ethylene–octene (EO) copolymer. These data are listed in Table 1, along with the deuterated linear HDPE-D used to provide SANS contrast. Mixtures with HDPE-D (80/20 for the EH and 75/25 for the EO copolymers) were prepared by dissolving the components (~ 300 mg) in 125 mL of *o*-dichlorobenzene and stirring at 178 °C for 15 min. The solution was rapidly quenched into 2 L of chilled methanol (~ -60 °C), and after filtering and washing with methanol, the crystals were dried overnight in a vacuum oven at 60 °C. Disks ≈ 1 mm thick were compression-molded in a Carver press at 190 °C and quenched into ice–water.

Small-Angle Neutron Scattering: Data Collection

The original experiments⁷ were performed on the W. C. Koehler 30 m SANS facility¹⁶ at the Oak Ridge National Laboratory via a 64×64 cm² area detector with cell (element) size ~ 1 cm² and a wavelength (λ) of 4.75 Å, in the Q range $0.0045 < Q = 4\pi\lambda^{-1} \sin \theta < 0.04$ Å⁻¹, where 2θ is the angle of scatter. Subsequently, this instrument has been shortened to an overall length of 12 m to create space for the construction of two new SANS facilities.¹⁷ This restricts the minimum Q value to $Q_{\min} \approx 0.007$ Å⁻¹, which is insufficient to resolve the dispersed phase.

We have therefore complemented these measurements with experiments on the KWS1 SANS facility¹⁸ at the FRJ2 research reactor in Jülich, which can access Q values down to 0.002 Å⁻¹. Both data sets were corrected for instrumental and incoherent backgrounds as described previously^{1,2,6–8} and normalized to an absolute ($\pm 4\%$) differential cross section per unit sample

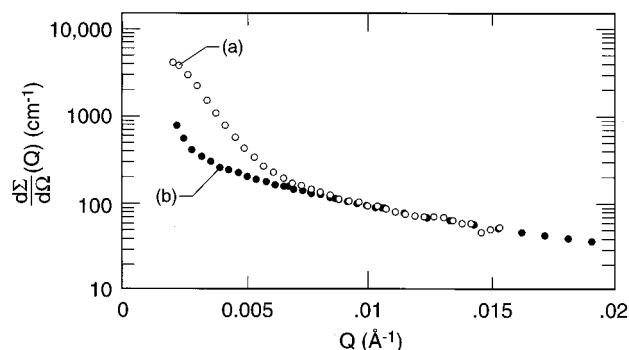


Figure 1. $d\Sigma/d\Omega(Q)$ for (a) 20/80 blend of HDPE-D and heterogeneous (Ziegler–Natta catalyzed) ethylene–hexene LLDPE copolymer blend (○) and (b) (25/75) blend of HDPE-D with a metallocene-based ethylene–octene copolymer (●).

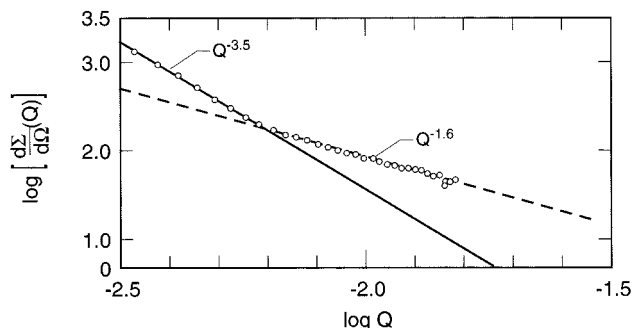


Figure 2. $\log [d\Sigma/d\Omega(Q)]$ vs $\log Q$ for 20/80 blend of HDPE-D with compositionally heterogeneous ethylene–hexene copolymer.

volume [$d\Sigma/d\Omega(Q)$ in units of cm⁻¹] by the same precalibrated secondary standards.¹⁹

Small-Angle Neutron Scattering: Data Analysis

Figure 1a shows the cross section in the melt ($T = 145$ °C), measured on the Jülich KWS1 spectrometer¹⁸ of the original commercial ethylene–hexene (EH) copolymer, prepared with a ZN catalyst and may be compared with the data taken at 160 °C on the ORNL 30 m facility [ref 6; Figure 1]. Despite the fact that the samples were run several years apart on different spectrometers at slightly different temperatures, there is good overlap between the data, and the exponent of the cross section $d\Sigma/d\Omega \sim Q^{-n}$ derived from the low- Q “upturn” is $n \approx 3.5$, compared to $n \approx 3.8$ measured previously.⁷ Figure 1b shows the melt cross section of the metallocene ethylene–octene copolymer measured on the KWS1 spectrometer.

The existence of multiple phases in the ZN copolymer is reflected in the SANS data, and this blend clearly exhibits two regions where the scattering varies as $Q^{-3.5}$ and $Q^{-1.6}$ for the lowest and highest Q values, respectively (Figure 2). These exponents are close to the Porod limit (Q^{-4} , for phases with sharp boundaries²⁰) and the Gaussian (Debye) coil limit (Q^{-2} , for individual random coil molecules^{21,22}). It was previously shown that xylene extraction, which removes the highly branched molecules, also removes the component which varies with the Porod exponent (-4), originating from the dispersed minority phase. This LLDPE has an average branch content of ~ 1.7 branches/100C, though a small fraction of the chains in the distribution are highly branched and phase separate from the lightly branched matrix.

As these molecules are incompatible with lightly branched chains, it is to be expected that they are also

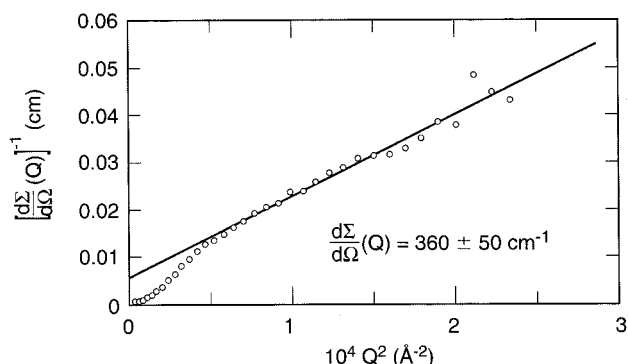


Figure 3. $[d\Sigma/d\Omega(Q)]^{-1}$ vs Q^2 for 20/80 blend of HDPE-D with heterogeneous ethylene-hexene LLDPE copolymer.

incompatible with the linear (deuterated) material which is added to provide SANS contrast. If these domains consisted of particles with relatively sharp boundaries, this would naturally give rise to the Q^{-4} variation observed in the low- Q (Porod) limit. Conversely, it is well-known¹⁻⁶ that lightly branched material is compatible with linear HDPE-D, so the matrix should consist of an homogeneous mixture of HDPE-D and LLDPE-H chains, and such a morphology would also give rise to the observed Q^{-2} variation over most of the Q range. Thus, the two-phase hypothesis¹²⁻¹⁴ accounts qualitatively for the general features of the scattering.

For a homogeneous blend of two polymer species, one of which is deuterium labeled, the coherent cross section is given^{1,23} by

$$\frac{d\Sigma}{d\Omega}(Q) = V^{-1}(a_H - a_D)^2[\phi_D N_D P_D(QR_{gD})]^{-1} + [(1 - \phi_D) N_H P_H(QR_{gH})]^{-1} - 2\chi]^{-1} \quad (1)$$

where a_D is the scattering length of the repeat unit (segment) of the labeled species (HDPE-D) and a_H is the scattering length of the unlabeled species (LLDPE-H). V is the segment volume, which is assumed to be the same for both species, as the vast majority of both components consists of C_2H_4 units. ϕ_D is the volume fraction of the labeled species, and R_{gD} , R_{gH} , N_D , and N_H are the radii of gyration and polymerization indices of the two species, with intramolecular chain functions $P_D(QR_{gD})$ and $P_H(QR_{gH})$ are represented by Gaussian (Debye) linear coils²¹⁻²³

$$P(Q, R_g) = 2[R_g^2 Q^2 + \exp(-R_g^2 Q^2) - 1]/(R_g^4 Q^4) \quad (2)$$

When $QR_g \gg 1$, the scattering is dominated by $P(Q, R_g)$, which varies as Q^{-2} in this limit (eq 2). χ is the Flory-Huggins interaction parameter, and for mixtures of protonated and deuterated HDPEs, the interaction arises from isotope effects,² with $\chi \approx \chi_{HD} \approx 4 \times 10^{-4}$, which is relatively independent of concentration for $0.2 < \phi_D < 0.8$. Similarly, for mixtures of linear and lightly branched molecules (<3 branches/100C), one of which is deuterated (e.g., HDPE-D/LLDPE-H), only the isotopic interaction parameter is observed via SANS.^{1,2} At small Q , the scattering may be described by the Ornstein-Zernicke (O-Z) equation^{1,2} $[d\Sigma/d\Omega(Q)]^{-1} = [d\Sigma/d\Omega(0)]^{-1}[1 + Q^2 \xi^2]$, where ξ is the composition fluctuation correlation length.

Figure 3 shows an O-Z plot $[d\Sigma/d\Omega(Q)]^{-1}$ vs Q^2 for the LLDPE-H/HDPE-D sample, where linear regression

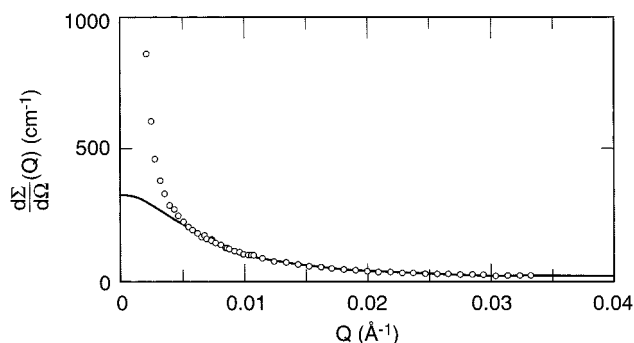


Figure 4. Fit to random phase approximation for 25/72 blend of HDPE-D with metallocene-based copolymer (omitting data below $Q < 0.01 \text{ \AA}^{-1}$).

omits the lowest Q region of the data. The forward ($Q = 0$) intercept is positive, as expected for a homogeneous mixture. Depending on the cutoff point chosen between the "Porod" and "Debye" regions of the data, the value is in the range $360 \pm 50 \text{ cm}^{-1}$, compared to $\approx 400 \text{ cm}^{-1}$ calculated from eq 4 with $\chi \sim \chi_{HD} \sim 4 \times 10^{-4}$. This supports the postulate that the vast majority of the sample forms a homogeneous mixture and the volume fraction of the minority ($\phi \sim 10^{-2}$) disperse phase can be estimated^{6,24} from the SANS invariant

$$Q_0 = \int_0^\infty Q^2 d\Sigma/d\Omega(Q) dQ = 2\pi^2 \phi_1 \phi_2 [\rho_1 - \rho_2]^2 \quad (3)$$

where ϕ_1 , ϕ_2 , ρ_1 , and ρ_2 are the volume fractions and scattering length densities of the phases.²⁴ The scattering from the minority phase is manifested (Figures 1a and 2) for $Q < 0.01 \text{ \AA}^{-1}$, where it is superimposed on the cross section of the majority of the sample consisting of an homogeneous mixture of HDPE-D/LLDPE-H. We have removed this coherent "background" by fitting the random phase approximation (eq 1) to the high- Q ($> 0.01 \text{ \AA}^{-1}$) portion of the data as shown in Figure 4 for the 25/75 HDPE-D/metallocene copolymer.

The random phase approximation (RPA) has previously been shown to work well for mixtures of linear and branched molecules where both components are either polydisperse¹ or monodisperse.^{3,4} However, in view of the difference in polydispersity between the branched ($M_w/M_n \approx 2.2$) and linear ($M_w/M_n \approx 5.4$) components, the RPA must be modified as discussed by Mori,²⁵ Weimann,²⁶ and co-workers, who described the polydispersity via a Schultz distribution. In the limit of $Q \rightarrow 0$, $P(Q)$ is no longer unity as in eq 2, but rather $(k + 1)/k$, where $k = [(M_w/M_n) - 1]^{-1}$. As $Q \rightarrow 0$, $P(Q) \rightarrow M_w/M_n$, and with this modification, the RPA fit is excellent for $Q > 0.01 \text{ \AA}^{-1}$. The R_g is a function of the segment length (a), and the fitted parameters [$a = (6/N)^{0.5} R_g \approx 5.8 \pm 0.1 \text{ \AA}$; $R_g/M_w^{0.5} \approx 0.45 \pm 0.01$; $\chi_{HD} \approx (3.1 \pm 1) \times 10^{-4}$] are similar to those previously reported.^{1,6,7,27-29} We have subtracted this function below $Q < 0.01 \text{ \AA}^{-1}$, and the net scattering is shown in the form of a Kratky plot [$Q^2 d\Sigma/d\Omega(Q)$ vs Q] in Figure 5.

However, we still have to estimate the portion of the area below $Q_{\min} \approx 0.002 \text{ \AA}^{-1}$, which must pass through the origin at $Q = 0$, and we assume that the missing data follow the Guinier approximation in the range $0 < Q < 0.002 \text{ \AA}^{-1}$. This leads to an estimate of the volume fraction of the disperse phase of $\phi \approx 0.030$, compared with $\phi \approx 0.021$ measured previously on the 30 m SANS instrument.⁷ In view of the fact that the scattering from

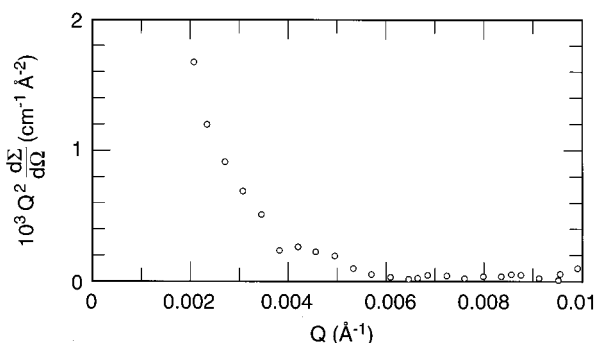


Figure 5. Invariant plot for low- Q upturn ($Q < 0.006 \text{ \AA}^{-1}$) from 25/75 blend of HDPE-D and metallocene-based copolymer after subtracting coherent background simulated by random phase approximation.

particles with dimensions $>3000 \text{ \AA}$ appears at Q values below the resolution limit of the previous experiment ($Q \approx 0.0045 \text{ \AA}^{-1}$), we have speculated that this was an underestimate in view of the fact that a portion of the invariant was experimentally inaccessible. We have subsequently used ultrahigh-resolution SANS (USANS) techniques³⁰ to fill in the missing portion of the data and improve the estimate to $\phi \approx 0.030$. Thus, USANS and the higher resolution KWS1-SANS substantially improve the estimate of ϕ by partially filling in the previously inaccessible portion of the SANS invariant.

The volume fraction of the disperse minority phase (0.03) from SANS is close to the value obtained in a similarly constituted ZN ethylene-1-butene copolymer by Nesarikar et al.,¹⁵ who carried out a thermodynamic calculation of the equilibrium liquid state using the multiphase equilibrium of multicomponent copolymers described by Bauer.³¹ The composition distribution was obtained from TREF and modified via an exponential tail to give the correct first moment, as measured by NMR. This led to a 3-fold increase in the composition variance and to the prediction of a two-phase melt for the heterogeneous copolymer, with a minority phase volume fraction (0.016) in agreement with microscopic analysis.

Our SANS analysis relies on addition of 20% deuterated linear polyethylene for SANS contrast, and thus, the composition variance of the blend differs from the pure ZN ethylene-1-hexene copolymer. This raises the possibility that the change in variance perturbs the melt phase structure, such that the information previously obtained⁷ by SANS from the HDPE-copolymer blend may not correspond to the pure ZN melt. We were not able to address this issue directly by duplicating the thermodynamic calculations of Nesarikar and co-workers,^{15,32} because TREF data were not available and the exact distribution of chain composition in the ZN ethylene-1-hexene copolymer was not known. However, the molecular weight, distribution, and overall branch content of the ZN copolymer of this study are very similar to those of the ethylene-1-butene studied by Nesarikar et al.,¹⁵ so it is reasonable to assume a similar comonomer composition distribution. This would lead to the same prediction of a dispersed minority phase in the melt, and in view of the close agreement between the observed⁷ and calculated^{15,32} volume fractions of the minority phase, it seems plausible that SANS data from the blend reflect the actual melt structure of the copolymer. In addition, the same volume fraction of the minority phase was obtained by extracting the highly branched molecules.⁷

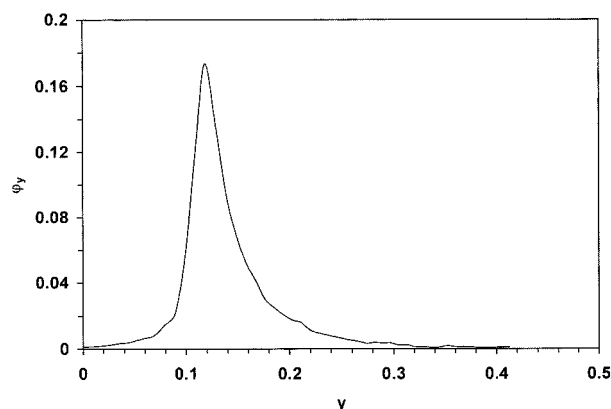


Figure 6. TREF composition distribution of metallocene ethylene-1-octene copolymer.

Figure 1b shows the SANS cross section of the blend of 25% HDPE-D with the metallocene-based ethylene-octene (EO) copolymer, and it may be seen that the division into "Porod" and "Debye" regions of the scattering as observed for the ZN-based copolymer does not apply for the homogeneous metallocene-catalyzed copolymer. The small upturn at very low Q values ($<6 \times 10^{-3} \text{ \AA}^{-1}$) probably arises from voids in the samples, which is a general feature of scattering from polymer blends.² However, most of the scattering associated with the "Porod" region in the ZN-based blend is absent in the metallocene-based mixture, which does not contain the highly branched molecules present in the ZN copolymer, and hence the scattering pattern does not exhibit a "Porod" region originating from a dispersed minority phase.

Regardless of the change in composition variance upon blending, the experimental SANS cross section data of Figure 1b are consistent with a melt phase structure that is not significantly altered from the pure copolymer's melt. The addition of the linear component leads to an increase of the original composition variance toward the spinodal condition, but distinctive details of phase-separated systems are absent in Figure 1b.

A more rigorous treatment to assess whether multiple equilibrium phases coexist in the liquid phase of the metallocene copolymer investigated and whether the addition of HDPE perturbs the melt structure can be obtained following the thermodynamic approach previously undertaken for model copolymers³² and for the heterogeneous Ziegler type.¹⁵ However, in view of the relatively low overall comonomer concentration and the narrow composition distribution of the metallocene-EO copolymer, reasonable predictions could be made on the basis of the spinodal condition ($\chi_{AB} = \chi_s$ where χ_{AB} is the interaction parameter of a polyethylene-poly-1-octene blend and χ_s the value corresponding to the spinodal condition).

The composition variance of the pure copolymer was calculated from TREF data of a matched copolymer, which is shown in Figure 6 and corresponds to an ethylene-1-octene copolymer obtained with the same metallocene catalyst under identical polymerization conditions to ensure a similar composition distribution. The average comonomer composition, measured by ^{13}C NMR, is 1.68 hexyl branches per 100 backbone carbons, similar to 1.5 mol % measured for the copolymer studied by SANS. The distribution of chain composition for the 25/75 blend was empirically simulated as shown in Figure 7. The distribution of the linear component was

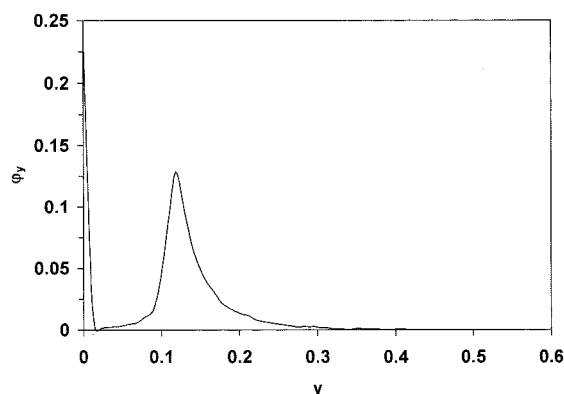


Figure 7. TREF composition distribution of 25/75 HDPE-D/metalocene EO blend. The linear component was empirically simulated as a lightly branched HDPE.

Table 2. Characteristics of Average Composition, Composition Variance, and Spinodal Condition for Pure Metalocene EO and 25/75 Blend with Deuterated Linear Polyethylene

polymer	\bar{y}	\bar{y}^2 (10^2)	$(\bar{y}^2 - \bar{y}^2)$ (10^3)	χ_s^a	χ_{AB}/χ_s
metalocene EO	0.144	2.35	2.75	0.24	0.13
25/75 blend	0.107	1.75	5.96	0.12	0.25

^a Calculated from eq 5.

approximated by a Gaussian function of lightly branched chains. The overall distributions are represented by a total of 55–60 components for both the pure copolymer and the blend. In these figures φ_y is the fraction of copolymers having composition y . Hence, $\sum_{y=0}^1 \varphi_y = 1$ and the average composition is $\bar{y} = \sum_{y=0}^1 y \varphi_y$.

The stability condition is given in a simplified form as³³

$$\chi_s N_w (\bar{y}^2 - \bar{y}^2) = \frac{1}{2} \quad (4)$$

where $(\bar{y}^2 - \bar{y}^2)$ is the compositional variance and $\bar{y}^2 = \sum_{y=0}^1 y^2 \varphi_y$. N_w is the weight-average degree of polymerization, which on the basis of octene repeats is taken as 754 for the copolymer and 804 for the blend and y is the fraction of branched repeats, calculated from the number of branches per 100 backbone carbons (x_b) as $y = 4x_b/(3x_b + 50)$. The calculated composition variance and the characteristics of the distribution for the pure copolymer and blend are given in Table 2. We may note that the variance is wider for the blend than the copolymer. Thus, if the addition of the HDPE-D homopolymer had perturbed the melt phase structure, it would have been in the direction of *phase separation*. As the main conclusion of this study is that the metalocene copolymer is *homogeneous*, this could not be an artifact caused by the addition of homopolymer, as any perturbation would have been in the opposite direction.

The same value of $\chi_{AB} = 0.03$ was used to calculate the ratio χ_{AB}/χ_s for the pure copolymer and the blend.^{15,34,35} This ratio gives useful qualitative information about proximity of the system to the spinodal decomposition ($\chi_{AB}/\chi_s = 1$). The calculated ratios, 0.13 for the pure metalocene EO and 0.25 for the blend, are far from the spinodal condition, indicative of melt homogeneity in agreement with the results from SANS. We should mention, parenthetically, that the average composition calculated from the TREF distribution of

the copolymer of Figure 6, $\bar{y} = 1.9$ hexyl branches per 100 backbone carbons, is an upper bound to the value measured by NMR of 1.68 mol %. In view of the many different causes for the discrepancy, i.e., off calibration, cocrystallization of chains with different composition that are eluted at the same temperature, retention of gels formed from lightly branched molecules, etc., we chose not to modify the TREF distribution to obtain the average NMR composition. Moreover, we should indicate that such modification would lead to a more symmetric distribution and to a decrease of the composition variance and, thus, to even lower χ_{AB}/χ_s ratios than those listed in Table 2.

We may estimate the possible error in the invariant (eq 6), caused by the low- Q upturn attributed to voids [Figure 1b; $Q < 6 \times 10^{-3} \text{ \AA}^{-1}$], as it is superimposed on the cross section of the majority of the sample consisting of a homogeneous mixture of HDPE-D and LLDPE-H. We have removed this coherent “background” by fitting the random phase approximation to the high- Q ($> 0.01 \text{ \AA}^{-1}$) portion of the data in the same way as for the heterogeneous ZN-catalyzed polymer, as both data sets superimpose for $Q > 0.01 \text{ \AA}^{-1}$. To estimate the portion of the area below $Q_{\min} \approx 0.002 \text{ \AA}^{-1}$, we again rely on the fact that the curve must pass through the origin at $Q = 0$ and assume that the missing low- Q data follow the Guinier approximation, to give an integrated area of $Q_0 \approx 3.3 \times 10^{-6} \text{ cm}^{-1} \text{ \AA}^{-3}$. This may be compared with $Q_0 \approx 47 \times 10^{-5} \text{ cm}^{-1} \text{ \AA}^{-3}$, which was used to estimate the volume fraction ($\phi \approx 0.030$) of the dispersed phase in the ZN-catalyzed sample (Figure 1a). Thus, the upturn that we have attributed to void scattering is a minor perturbation ($< 1\%$) in the determination of the volume fraction of the dispersed phase.

These findings indicate that the metalocene copolymer molecules are mixed homogeneously within a single phase and support previous conclusions⁷ concerning liquid–liquid phase separation for compositionally polydisperse LLDPEs, whereby the highly branched molecules in the distribution phase segregate, even if the overall branch content is low. This research is relevant to the understanding of the melt phase behavior of ethylene copolymers, though effect of the presence or absence of such a disperse phase on the fracture toughness of LLDPE remains to be established by independent studies.

Acknowledgment. The research at Oak Ridge was supported by the Laboratory Directed Research and Development Program and by the Division of Materials Sciences, under Contract DE-AC05-00OR22725 with the Oak Ridge National Laboratory, managed by UT-Battelle, LLC. The work at the FAMU-FSU College of Engineering was supported by the National Science Foundation Polymer Program (DMR 009448594), whose aid is gratefully acknowledged. E.J.R. worked under the Research Experiences for Undergraduates program of the NSF. G.D.W. thanks Professor D. Richter for the hospitality of the Forschungszentrum and the assistance provided by the staff of the IFF.

References and Notes

- (1) Alamo, R. G.; Londono, J. D.; Mandelkern, L.; Stehling, F. C.; Wignall, G. D. *Macromolecules* **1994**, *27*, 411.
- (2) Londono, J. D.; Narten, A. H.; Wignall, G. D.; Honnell, K. G.; Hsieh, E. T.; Johnson, T. W.; Bates, F. S. *Macromolecules* **1994**, *27*, 2864.

- (3) Graessley, W. W.; Krishnamoorti, R.; Balsara, N. P.; Fetters, L. J.; Lohse, D. J.; Schultz, D. N.; Sissano, J. A. *Macromolecules* **1994**, *26*, 1137; **1994**, *27*, 2574, 3073, and 3896.
- (4) Krishnamoorti, R.; Graessley, W. W.; Balsara, N.; Lohse, D. J. *Macromolecules* **1994**, *27*, 3073.
- (5) Nicholson, J. C.; Finerman, T.; Crist, B. *Polymer* **1990**, *31*, 2287. Rhee, J.; Crist, B. C. *Macromolecules* **1991**, *24*, 5665.
- (6) Alamo, R. G.; Graessley, W. W.; Krishnamoorti, R.; Lohse, D. J.; Londono, J. D.; Mandelkern, L.; Stehling, F. C.; Wignall, G. D. *Macromolecules* **1997**, *30*, 561.
- (7) Wignall, G. D.; Londono, J. D.; Alamo, R. G.; Mandelkern, L.; Stehling, F. C. *Macromolecules* **1996**, *29*, 5332.
- (8) Wignall, G. D.; Alamo, R. G.; Londono, J. D.; J. S. Lin, L. Mandelkern, M. H. Kim and, G. M. Brown *Macromolecules* **2000**, *33*, 551.
- (9) Agamalian, M. M.; Alamo, R. G.; Kim, M. H.; Londono, J. D.; Mandelkern, L.; Wignall, G. D. *Macromolecules* **1999**, *32*, 3093.
- (10) Tashiro, K.; Imanishi, K.; Izuchi, M.; Kobayashi, M.; Itoh, Y.; Imai, M.; Yamaguchi, Y.; Ohashi, M.; Stein, R. S. *Macromolecules* **1995**, *28*, 8484.
- (11) Karbasheski, E.; Kale, L.; Rudin, A.; Tchir, W. J.; Cook, D. G.; Pronovost, J. *Appl. Polym. Sci.* **1992**, *44*, 425.
- (12) Schouteren, P.; Groeninckx, G.; Van der Heijden, B. V.; Jansen, F. *Polymer* **1987**, *28*, 2099.
- (13) Mirabella, F. M.; Ford, E. A. *J. Polym. Sci., Polym. Phys. Ed.* **1987**, *25*, 777. Mirabella, F. M.; Westphal, S. P.; Fernando, P. L.; Ford, E. A.; Williams, J. *J. Polym. Sci.* **1988**, *B26*.
- (14) Debliek, R. A. C.; Mathot, V. B. F. *J. Mater. Sci., Lett.* **1988**, *7*, 1276.
- (15) Nesarikar, A.; Crist, B.; Davidovich, A. *J. Polym. Sci.* **1994**, *B32*, 641.
- (16) Koehler, W. C. *Physica (Utrecht)* **1986**, *137B*, 320.
- (17) See <http://neutrons.ornl.gov/NSatHFIR/Upgrades/HFIRUp-Fac.HTML>.
- (18) *18. Neutronenstreuexperimente am FRJ2 in Jülich*, 1997 (English and German texts are available from the Forschungszentrum, Jülich).
- (19) Wignall, G. D.; Bates, F. S. *J. Appl. Crystallogr.* **1986**, *20*, 28.
- (20) Porod, G. In *Small-Angle X-ray Scattering*; Glatter, O., Kratky, O., Eds.; Academic Press: New York, 1982; Chapter 2, p 30.
- (21) Debye, P. *J. Appl. Phys.* **1944**, *15*, 338.
- (22) Flory, P. J. *Principles of Polymer Chemistry*; Cornell University Press: Ithaca, NY, 1969; p 295.
- (23) deGennes, P. G. In *Scaling Concepts in Polymer Physics*; Cornell University Press: Ithaca, NY, 1979; Chapter 5.
- (24) Wignall, G. D. In *Polymer Properties Handbook*; Mark, J. E., Ed.; American Institute of Physics: Melville, NY, 1996; p 299.
- (25) Mori, K.; Tanaka, H.; Hasegawa, H.; Hashimoto, T. *Polymer* **1989**, *30*, 1389.
- (26) Weimann, P. A.; Jones, T.; Hillmyer, M. A.; Bates, F. S.; Londono, J. D.; Melnichenko, Y.; Wignall, G. D.; Almdal, K. *Macromolecules* **1997**, *30*, 3650.
- (27) Wignall, G. D. In *Encyclopedia of Polymer Science and Engineering*; Grayson, M., Kroschwitz, E. M., Eds.; Wiley and Sons: New York, 1987; Vol. 10, p 112.
- (28) Lieser, G.; Fischer, E. W.; Ibel, K. *J. Polym. Sci., Polym. Lett. Ed.* **1975**, *28*, 39.
- (29) Boothroyd, A. T.; Rennie, A. R.; Boothroyd, C. B. *Europhys. Lett.* **1991**, *15*, 715.
- (30) Agamalian, M. M.; Alamo, R. G.; Londono, J. D.; Stehling, F. C.; Mandelkern, L.; Wignall, G. D. *Mater. Res. Soc. Symp. Proc.* **1997**, *461*, 205.
- (31) Bauer, B. J. *Polym. Eng. Sci.* **1985**, *5*, 1081.
- (32) Nesarikar, A.; Olvera de la Cruz, M.; Crist, B. *J. Chem. Phys.* **1993**, *98*, 7385.
- (33) Scott, R. L. *J. Polym. Sci.* **1952**, *9*, 423.
- (34) Rhee, J.; Crist, B. *Macromolecules* **1991**, *24*, 5663.
- (35) Rhee, J.; Crist, B. *J. Chem. Phys.* **1993**, *98*, 4174.

MA0106970